

H₂-Rich Interstellar Grain Mantles: An Equilibrium Picture

Richard W. Dissly¹, Mark Allen^{1,2}, and Vincent G. Anicich²

Submitted to: *The Astrophysical Journal*, March 14, 1994

26 Pages

5 Figures

¹ Division of Geological and Planetary Sciences, California Institute of Technology,
MS 170-25, Pasadena, CA 91125

² Earth and Space Sciences Division, Jet Propulsion Laboratory, California Institute of
Technology, MS 183-601, 4800 Oak Grove Drive, Pasadena, CA 91109

ABSTRACT

Experiments simulating the codeposition of molecular hydrogen and water ice on interstellar grains demonstrate that amorphous water ice at 12 K can incorporate a substantial amount of H₂, up to a molar ratio of H₂/H₂O = 0.53. We find that the physical behavior of ~80% of the hydrogen can be explained satisfactorily in terms of an equilibrium population, thermodynamically governed by a wide distribution of binding site energies. Such a description predicts that gas phase accretion could lead to fractional molar abundances of H₂ in interstellar grain mantles of nearly 0.3; for the probable conditions of W1.5 in the p Ophiuchi cloud, fractional H₂ abundances of between 0.05 and 0.3 are predicted, in possible agreement with the observed abundance reported by Sandford, Allamandola, & Geballe (1993). Accretion of gas phase H₂ onto grain mantles, rather than photochemical production of H₂ within the ice, could be a general explanation for frozen H₂ in interstellar ices. We speculate on the implications of such a composition for grain mantle chemistry and physics.

1. INTRODUCTION

Although molecular hydrogen is produced catalytically on grain surfaces in the interstellar medium, the amount of frozen H₂ present in grain mantles is uncertain. The extreme volatility of H₂ qualitatively suggests that very low temperatures are required for an appreciable amount of H₂ to condense on a grain surface. However, if a significant fraction of an icy grain mantle at realistic interstellar cloud temperatures were to consist of H₂, it would have a major impact on grain surface chemistry and gas-grain interactions (see, for example, Allen & Robinson 1976, 1977). The present paper is an extension of experimental work presented earlier (Dissly, Allen, &

Anicich 1992), which reported that a large fraction of molecular hydrogen could be incorporated in interstellar water ice grain mantles under typical molecular cloud conditions by codepositional accretion of gas phase H_2 with H_2O . This is important in light of the recent detection of frozen H_2 in interstellar ice in the infrared spectrum of WL5, a deeply embedded protostar in the ρ Ophiuchus molecular cloud complex (Sandford et al. 1993).

Much speculation has been made in the past about the possibility of growing H_2 mantles on interstellar grains. Early estimates of the likelihood of H_2 condensation relied on vapor pressure studies (Wickramasinghe & Reddish 1968; Solomon & Wickramasinghe 1969; Lee, Gowland, & Reddish 1971). These results suggested that a thick H_2 mantle was possible only for temperatures ≤ 4 K. Subsequent reports have been in terms of the binding energy, E_b , of H_2 to various surface compositions. As grain surfaces are thought to be covered by an icy mantle composed largely of amorphous water ice (see, for example, Tielens & Allamandola 1987), most studies have specifically addressed the binding energy of H_2 to solid H_2O . Early predictions of E_b for the physisorption of H_2 range from a theoretical estimate of 550 K (Hollenbach & Salpeter 1970) to a higher experimental value of 860 K (Lee 1972), where E_b is given in units of temperature, i.e., energy divided by Boltzmann's constant. The most recent experimental value of the H_2 - H_2O binding energy is 555 ± 35 K (Sandford & Allamandola 1993).

The rate of growth of an adsorbed H_2 layer on a grain surface can be predicted by comparing the rate of collision between gas phase H_2 and a grain, assuming a unit sticking efficiency, with the residence time for the H_2 to remain bound to a grain surface. The residence time scale of an adsorbed molecule is described by the Arrhenius expression

$$\tau_{\text{res}} \sim \tau_{\text{vib}} \exp[E_b/T], \quad (1)$$

where T is the grain temperature and τ_{vib} is the vibrational period of the adsorbed molecule in its binding site on the surface ($\sim 10^{-13}$ s for 112-112C); Sandford & Allamandola 1993). For the 112-1120 binding energies given above, this expression predicts that H_2 would condense out on grain surfaces for typical interstellar cloud temperatures and H_2 gas number densities. However, the binding energy of H_2 to an H_2 surface is known to be quite small, ~ 100 K (Lee 1972). For this low value of the binding energy, the residence time scale for H_2 is substantially shorter than the collision time scale for conceivable interstellar conditions. Thus the growth of a pure H_2 mantle is self limiting, as the binding energy of H_2 to the grain surface will decrease as the H_2 coverage increases. The point at which an equilibrium coverage occurs for given interstellar conditions is quite sensitive to the H_2 surface binding energy to the water ice. Estimates of this equilibrium coverage range from an H_2 layer a few monolayers thick (Lee 1972) to a single H_2 monolayer covering only $\sim 20\%$ of the grain surface (Govers, Materna, & Scoles 1980; Tielens & Hagen 1982).

As a variation on the theme of condensation, H_2 may accumulate in the mantle at a significant level as it coaccretes with other mantle species, such as H_2O . This is a more realistic model of mantle growth, as species will collide with grain surfaces at rates proportional to their respective gas phase abundances. Previous codepositional experiments of H_2 with H_2O showed that the amount of hydrogen incorporated in a water matrix could be substantial, with a molar ratio of $\text{H}_2/\text{H}_2\text{O}$ as high as 0.63 (Laufer, Kochavi, & Bar-Nun 1987). This result suggests that H_2 may be a significant component throughout the volume of an icy grain mantle, and not just on the grain surface.

Accretion of H_2 from the gas phase is not the only way to incorporate molecular hydrogen into an icy grain mantle. Recent experiments have shown that molecular hydrogen can be chemically produced within the ice by the ultraviolet photolysis of mantle species that are rich in hydrogen, such as H_2O or C_2H_2

(Sandford & Allamandola 1993). These experiments have shown that for laboratory ice mixtures thought to typify interstellar grain mantle compositions, the fractional molar abundance of H₂ relative to H₂O saturates at ~0.35, limited by the availability of hydrogen in the system. In addition, the product H₂ is apparently either trapped or bound strongly enough in the ice that it does not effectively sublime below 30 K, and can be detected in the ice mixture even at temperatures as high as 70 K.

A more detailed understanding of the relative importance of the different physical processes that may result in the incorporation of H₂ in amorphous water ice is needed to properly model the composition of grain mantles in various interstellar environments. To that end, this paper reports the results of an experimental investigation of the composition and physics of ice samples prepared by codepositing amorphous water ice with an excess amount of H₂. We conclude that codepositional accretion of H₂ is a possible general mechanism for incorporating large amounts of molecular hydrogen in interstellar icy grain mantles.

2. EXPERIMENTAL PROCEDURE

For this report, we have utilized an experimental arrangement similar to that described elsewhere (Allamandola, Sandford, & Valero 1988). Briefly, the apparatus consists of two differentially pumped chambers, which are each evacuated by a turbomolecular pump (Balzers TPU170) to a background pressure of $\sim 3 \times 10^{-8}$ torr. Extending into the first chamber is a closed cycle helium refrigerator (Air Products Displex DE-202), which can be cooled down to 12 K. Attached to the end of the refrigerator is a sapphire window. The temperature of the window can be varied from 12 K to room temperature, with an accuracy of ± 0.2 K, by a resistive heater at the base of the window, monitored by a gold-chromel thermocouple and maintained by a temperature control system (Scientific instruments Series 5500). Ice samples

were prepared by simultaneously spraying H_2 and H_2O from separate gas lines slowly onto the cooled window. The gases were sprayed from pinholes 0.06 mm in diameter, set 4.0 cm away from the window. The composition of each ice sample was characterized upon heating by a quadrupole mass spectrometer (Extrel), housed in the second, adjacent vacuum chamber. Transmittance spectra were taken of the ice samples with a Fourier Transform infrared Spectrometer (Mattson Cygnus 25) between 2000 and 5000 cm^{-1} at a resolution of up to 1 cm^{-1} .

Recent experimental work on the structure of vapor-deposited amorphous water ice indicates that the surface area of the ice is highly dependent on the deposition conditions (Mayer & Pletzer 1986). Consequently, we tried to control our deposition parameters to simulate the interstellar accretion of icy mantles as closely as possible. The structure resulting from the slow growth of interstellar ice mantles can effectively be reproduced in the laboratory using depositions with a Knudsen number > 1 ($K_n =$ ratio of mean free path of gas in reservoir to nozzle diameter). This gives depositional flow in the molecular rather than supersonic regime. The resulting low growth rate yields an ice with a high surface area, due to a microporous structure with pore sizes typically $< 20 \text{ \AA}$ (Mayer & Pletzer 1986). Our experimental nozzle backing pressures of between 0.05 torr and 1.2 torr were purposefully kept low, such that K_n was between 1.2 and 12. The deposition rate of the water sample was approximately 0.2 - 0.5 $\mu\text{m/hr}$, measured by monitoring the interference fringes from a HeNe laser reflected from the growing sample. Our ice samples were transparent, indicating no structure within the ice larger than $\sim 1000 \text{ \AA}$.

1 Depositions were carried out for several window temperatures between 12 and 30 K. Deposition times ranged between 20 minutes and 2.5 hours. To assure that the relative gas collision rate of H_2 with the growing ice was greater than that of H_2O , as is the situation in interstellar molecular clouds, ice samples were prepared with relative gaseous $\text{H}_2:\text{H}_2\text{O}$ inlet pressures of between 4:1 and 36:1. The slow deposition

of water did not affect the ambient pressure in the chamber, indicating that most of the input water molecules immediately condensed out on the window. This was not the case with the input of H_2 . Admission of H_2 into the vacuum chamber raised the chamber pressure from the background of $\sim 3 \times 10^{-8}$ torr to $\sim 1 \times 10^{-5}$ torr. The deposition of an ice sample can then be viewed as the growth of H_2O in the presence of a surrounding 10^{-5} torr atmosphere of H_2 .

Once the deposition was completed, the sample was allowed to sit ~ 10 minutes, until the pressure in the chamber had dropped, and re-equilibrated. The sample was then heated, typically at a rate of 2 K/rein. The evolved gases were monitored with the mass spectrometer, calibrated to the absolute partial pressures of both H_2 and H_2O . We derived the rate of gas release from the sample with the following formula,

$$\text{Desorption Rate [molec/min]} = \frac{\text{Pumping speed [l/rein]} * \text{Number density [molec/l]}}{\text{Number of molecules per unit volume}} \quad (2)$$

with the number density of each gas determined from the mass spectrometer reading, and pumping speeds (100 l/s for H_2O , and 66 l/s for H_2) given by the pump manufacturer. Integrating this rate over the time it took for the entire ice sample to sublimate gave the total abundance of H_2 and H_2O in the sample.

Care was taken to account for the cryopumping of water ice from our samples on the cold refrigerator column above the window during the sample heating. This was done by observing the ratio of chamber pressures due to the injection of water with the full system at room temperature, versus the system with the refrigerator cold, but with a window temperature of 200 K, so that no ice would condense directly on the window. This calibration procedure was repeated several times, giving a ratio of warm/ /cold of 6.4 ± 0.1 , meaning that the large majority of water molecules liberated during the sample sublimation condensed out on the upper refrigerator

column. The amount of water seen by the mass spectrometer was thus underrepresented by a factor of 6.4 ± 0.1 , so our water measurements were scaled by this amount to give the total amount of water in the ice samples. The same procedure indicated that the cryopumping of H_2 is negligible.

3. RESULTS

In our initial experiments, the sapphire window onto which the ice samples were deposited was cooled to 12 K, a typical dark cloud grain temperature. The ice samples were prepared with relative gaseous $\text{H}_2:\text{H}_2\text{O}$ inlet pressures of up to 36:1, as described in the experimental section. Different sample thicknesses of ice were grown by varying the deposition times. The total abundances of H_2 and H_2O for each ice sample prepared, found by integrating under the desorption profiles for each species during sample heating, are summarized in Figure 1. It is immediately evident that amount of hydrogen in our samples correlates with the total amount of water in the sample. A linear regression through the data yields a best fit for the ratio $\text{H}_2/\text{H}_2\text{O}$ of 0.53. Given our uncertainties, this is in good agreement with the $\text{H}_2/\text{H}_2\text{O}$ value of 0.63 found in the codepositional experiments of Laufer et al. (1987), although their deposition rates were significantly faster than ours. Although the ice samples were prepared with relative $\text{H}_2:\text{H}_2\text{O}$ gas inlet rates of between 4:1 and 36:1, the $\text{H}_2/\text{H}_2\text{O}$ ratio in our ice samples did not depend on this ratio in any systematic way, suggesting that the maximum amount of hydrogen that can be incorporated in the ice is quickly reached for a small excess of H_2 over H_2O .

Depositing only H_2 onto the 12 K window for 1 hour yielded very little hydrogen upon heating (Fig. 1, open diamond), confirming that H_2O ice is the substrate responsible for the H_2 binding. A similar 1 hour deposition of pure H_2O

also produced negligible H_2 when the ice was heated (Fig. 1, open circle), demonstrating that the H_2 detected in our experiments is not a decomposition product of the H_2O in the ionizing region of the mass spectrometer. Residual water and hydrogen in the system over the course of the experiments made repeatability difficult. This uncertainty in the measurements is represented by the scatter of the data.

Since the ice samples were grown on the coldest point of the refrigerator, we were concerned about the possibility of H_2O cryopumping onto our sample from other parts of the chamber during the sample resorption, and perhaps affecting the measured ratio in the process. We therefore ran two control experiments: letting the ice sample sit in the chamber for several hours under vacuum at the end of the deposition (Fig. 1, open triangle), and letting the sample sit for several hours after the deposition under a 10^{-5} torr atmosphere of H_2 (Fig. 1, open square). This waiting period was hopefully long enough so that the cryopumping of additional H_2O on our sample would have become negligible. The former run represents the lowest extreme of $112/112\text{CJ}$ in our codeposited samples, suggesting that some cryopumping of H_2O was occurring after the deposition had ended. The latter experiment alternatively yielded the highest $\text{H}_2/\text{H}_2\text{O}$ ratio of our codepositions, as even the cryopumped water was deposited under a large excess of H_2 . Consequently, the brief waiting period between the end of deposition and the beginning of desorption in all our other experiments may have resulted in a final layer of deposited H_2O not saturated with H_2 . Therefore, our derived fit of $112/112\text{CJ} = 0.53$ may be a lower limit to the true saturated value at 12 K.

The typical temperature programmed desorption (TPD) profiles for both H_2 and H_2O are shown in Figure 2, for depositions at window temperatures of 12, 20, and 30 K. For each ice sample, the hydrogen and water mixtures were deposited at the same rate (inlet nozzle backing pressures of 0.8 and 0.2 torr, respectively), and for

the same duration (70 minutes), and in each case the heating progressed at a steady rate of 2 K/min. The total amount of H_2 and H_2O in our samples was found by integrating under the desorption curves. The relative ratios of the total H_2 in each sample for the different deposition temperatures are 12:20:30 K -100:37:4, showing a significant decrease with increasing substrate temperature. Close inspection of the H_2 desorption profile for the 12 K deposition shows two distinct regions: a low temperature component, represented by the large peak below -30 K in which the majority (~80%) of the total hydrogen leaves the sample, and a high temperature component, represented by the broad plateau of a lower hydrogen liberation rate from -30-80 K. The 20 K deposition has a similar structure, although less total H_2 . Our desorption profiles are similar to results reported previously (Laufer et al. 1987; Sandford & Allamandola 1993). We will contrast the explanations for the structure in the profiles later in this paper.

To investigate whether the high temperature component of the 12 K deposition shown in Figure 2 was not simply due to the time-delayed diffusion of unbound hydrogen from deeper layers in the ice, we performed the TPD experiment shown in Figure 3. The deposition conditions were identical to those given for the depositions in Figure 2. The ice sample was heated at the rate of 2 K/min, except when the temperatures were 20, 30, and 40K, at which times the temperature was held constant for approximately 10 minutes to allow for the complete release of any labile H_2 in the sample volume. During the 10 minute temperature holds, the H_2 release rate dropped quickly to the background level. When we resumed increasing the sample temperature, the H_2 release rate immediately returned to the value when the increase in temperature was halted. We conclude from this that time-delayed solid-state diffusion of deeply bound H_2 is not significant. In fact, diffusion may not be the factor controlling the release of H_2 from the ice at all. Our results are consistent with the H_2 stable in the water ice at high temperatures. If this is true,

then the respective areas under each temperature interval represent the amount of H_2 stably bound within that interval. The fraction of H_2 left in the water ice at each temperature arc: $T > 12$ K, 1.0; $T > 20$ K, 0.37; $T > 30$ K, 0.19; and $T > 40$ K, 0.15.

Finally, we took transmittance spectra of the ice samples from 2000 to 5000 cm^{-1} at a nominal resolution of 1.0 cm^{-1} . Previous authors have reported an induced H_2 vibrational feature at 4137 cm^{-1} (Ilxson et al. 1992; Sandford & Allamandola 1993) for frozen 112-1120 mixtures, but we did not detect anything in this spectral region. As our samples were only ~ 0.5 μm thick, such a feature would be quite weak. We assign an upper limit to the integrated band absorbance A of $< 1.8 \times 10^{-19}$ $\text{cm}/\text{molecule}$ for any feature at or near 4137 cm^{-1} . This is done by correlating the measured 112/1120 ratio in our samples with the integrated absorbance of the observed 3.1 μm water ice peak. This is consistent with a previous estimate of the integrated absorbance for the H_2 band of $A > (9.4 \pm 0.9) \times 10^{-20}$ (Sandford & Allamandola 1993).

4. PHYSICAL DESCRIPTION OF H_2 INCORPORATION IN WATER ICE

The recent detection of molecular hydrogen in interstellar ices raises a fundamental question: is the detected H_2 a product of photochemical reactions within an ice of hydrogen containing compounds such as water or methanol, as suggested in the experiments of Sandford & Allamandola (1993), or is the hydrogen simply the result of incorporation of ambient gas phase H_2 during the growth of grain mantles in the molecular cloud? Taken at face value, our laboratory results would suggest that codepositional adsorption alone could yield H_2 as a major component in interstellar grain mantles. However, the experimental conditions and time scales in our laboratory are quite different than those in the interstellar medium. To properly assess how our results can be applied to interstellar grain

mantles, we need a thorough understanding of the physical processes that govern the adsorption and growth of the ice samples in our experiments.

As shown previously in (I), the residence time scale for H_2 to remain in a physisorption site is governed by the binding energy, E_b . Theoretical and experimental values of the binding energy of H_2 to H_2O ice, typically in the context of surface adsorption, were given in the introduction. However, these reports each provide only a single value for the surface binding energy. In actuality, an amorphous ice has an irregular surface with physisorption sites having a *distribution* of binding energies. A recent computational study by Hixson et al. (1992) predicts what such a distribution might look like, determined by finding the potential minima of an isolated H_2 molecule on the model surface of an amorphous ice water cluster. The model provides a limited description of our experimental ices, as the surface potentials of a cluster can only approximate those of a macroscopic solid. In addition, the model does not take into account either the effects of the adsorbed H_2 on the structure of the water cluster or the adsorbed H_2 - H_2 interaction. Still, it does yield values for the H_2 surface binding energies that are reasonable in the context of previous theoretical and experimental reports. For a cluster of 450 water molecules, 240 possible surface binding sites for H_2 were found, with binding energies ranging in value from 320 K to 1399 K, with a peak in the population distribution at 650 K. In this theoretical distribution, 650 K is the most likely value for the binding energy. This is what the previous list of reported single-valued surface binding energies represents. The agreement between the peak of the theoretical distribution and the reported experimental values of 555 ± 35 K given by Sandford & Allamandola (1993) is good, given the limitations of the model calculation.

How might the concept of a distribution of binding site energies modify our thinking about H_2 incorporation in ices? The standard description of a single value for the surface binding energy predicts a uniform residence time scale for a given

adsorbed species. An ice surface that has a distribution of binding site energies will have a corresponding distribution of residence time scales. Given a collision rate of an adsorbable species like H₂, this distribution will dictate an equilibrium surface population such that sites with $\tau_{\text{res}} > \tau_{\text{col}}$ will always be filled by H₂, assuming that the sticking probability of an H₂ molecule with a grain surface is unity. The collision time scale for an H₂ molecule to encounter a particular binding site is given by

$$\tau_{\text{col}} \sim [n(\text{H}_2)_{\text{gas}} \sigma_{\text{site}} v_{\text{gas}}]^{-1}. \quad (3)$$

Equating (1) and (3) for a constant gas-phase collision rate and grain surface temperature gives a critical value of E_{b} such that all sites with $E_{\text{b}} > E_{\text{b}}(\text{crit})$ will always be filled by H₂ molecules.

This simple calculation actually provides an upper limit to the value of $E_{\text{b}}(\text{crit})$, as it only takes into account impinging gas phase H₂ as the source for molecular hydrogen. An additional source of H₂ is on the surface of the ice itself, as an adsorbed H₂ molecule is more likely to migrate over the surface than escape it completely. This is due to the fact that the kinetic barrier to migration to a neighboring site is roughly half the value of E_{b} , the barrier to escape from the surface (Tielens & Hagen 1982). One can then imagine a sort of “musical chairs” of H₂ among surface binding sites, with stronger sites preferentially occupied over weaker sites. Migration from weaker sites to their stronger counterparts provides a flux of H₂ to strong sites in addition to the gas phase flux, which will lower the level of the critical binding energy from that found with gas phase adsorption as the sole source of H₂.

The results shown in Figure 3 provide a test of whether the incorporation of H₂ in our laboratory ices can be described by such an equilibrium physical model. By assuming that the H₂ release in this TPD experiment is controlled only by

thermodynamic equilibrium, an experimental distribution of H_2 binding site energies can be inferred. The value of $E_b(\text{crit})$ for each of the temperature holds at 20, 30, and 40 K, and the initial temperature at 12 K, can be found as outlined above, by equating the H_2 collision rate with the residence time scale at that temperature. Since we are assuming that the ice sample is always in equilibrium, the collision rate of H_2 is dictated by the background pressure of H_2 when the sample is being heated, rather than the H_2 pressure during deposition. As the background pressure was $\sim 3 \times 10^{-8}$ torr, the H_2 number density was $\sim 1 \times 10^9 \text{ cm}^{-3}$. Thus, with a typical binding site size of 10^{-15} cm^2 , and with a gas temperature of 300 K, $\tau_{\text{col}} \sim 5$ seconds for an H_2 molecule to collide with an individual surface site under the background pressure. If we then take this 5 seconds as the residence time scale, and an ice temperature of 12 K, solving for $E_b(\text{crit})$ gives 380 K. Therefore, when our ice sample is sitting under a background pressure of H_2 at 12 K, all H_2 in binding sites with $E_b > 380 \text{ K}$ will have a longer residence time than it takes for a new H_2 molecule to find and occupy that site, and will always be filled by H_2 . If the H_2 population of our ice samples is truly governed by this equilibrium model, then only hydrogen in those binding sites with $E_b < E_b(\text{crit})$ will be labile at a given temperature hold in the TPD experiment. Repeating this simple procedure, the fraction of H_2 left in the water ice at 12, 20, 30, and 40 K then yields the relative number of sites in our sample with $E_b > E_b(\text{crit})$ for each of these temperatures.

The experimentally inferred relative distribution of binding sites with E_b greater than a given value from the Figure 3 TPD experiment are compared in Figure 4 with the results of the theoretically computed distribution by Hixson et al. (1992). Because the 12 K ice sample was allowed to sit for several minutes under the background pressure of H_2 immediately after the deposition, hydrogen in sites with $E_b < 380 \text{ K}$ escaped the sample before the measurements were started, so the experimental distribution is normalized to the theoretical one at 380 K. The

approximate agreement between the two distributions supports the physical picture of H_2 incorporated in the ice by the equilibrium distribution outlined above.

This physical model is applicable to ices deposited at temperatures above 12 K as well. This is shown by displaying in Figure 4 the relative amounts of H_2 in the samples deposited at 12, 20, and 30 K, discussed previously with reference to Figure 2. This data curve is normalized to the theoretical curve as before. Again, the relative abundances of the total H_2 in ices deposited at different temperatures is consistent with an equilibrium distribution of binding site energies.

Figure 4 shows additional interesting information. Although the overall fit of the theoretical distribution to the data is fair, the TPD experiment from Figure 3 shows a definite high energy tail, suggestive of H_2 from deeply buried sites not predicted by the theoretical surface model. These buried sites only appear to account for ~20% of the total number of sites, when compared to the theoretical distribution. As mentioned previously, the desorption profiles for the 12 K depositions, as shown in Figure 2, consist of two distinct regions with relative sizes that appear to be independent of the sample thickness: the main low energy peak, and a smaller, higher energy plateau. The plateau region accounts for ~20% of the total liberated H_2 in our 12 K deposited desorption profiles as well, suggesting that it is due to the desorption from deeply buried sites. The desorption profiles of very thin (~100 Å) ice samples (not shown) are a notable exception, as the plateau region appears to decrease in relative size as the samples decrease in thickness, although the H_2 desorption signal is very weak for samples this small. We therefore suggest that the primary peak in the H_2 desorption profile is due to the liberation of surface or near surface H_2 , in equilibrium with the gas phase, controlled by a distribution of binding energy sites similar to the theoretical one. The plateau is apparently due to deeply buried H_2 , either trapped in the water ice matrix or strongly bound by very energetic sites not described in the theoretical surface distribution by Hixson et al. (199?). Thus, in

our experiments, ~80% of the H_2 population is adequately described by the theoretical surface binding energy distribution, while ~20% is apparently due to H_2 buried deeply within the H_2 matrix. This is consistent with the results of the photochemical experiments by Sandford & Allamandola (1993). As the H_2 in their experiments was primarily produced deep within the volume of the ice rather than on or near the surface, this would explain their report that the total abundance of H_2 in their ice samples did not change significantly for temperatures less than 30 K. Our finding that this non-equilibrium H_2 is released from the ice at temperatures as high as 70 K is also consistent with their report.

The difference in the distribution between the two experimental curves in Figure 4 suggests that the amount of H_2 in the ice when it was deposited at 12 K and then raised to a certain temperature is systematically higher than when the ice is actually deposited at that same temperature. This difference may also be due to the burial of H_2 into deeper, more strongly bound sites. This is not surprising, as the 12 K deposition has a higher equilibrium surface abundance than a higher temperature deposition, allowing proportionally more H_2 to be buried into the non-equilibrium population as the water ice is growing.

It is interesting that the desorption profiles for a given deposition temperature appear to be independent of sample thickness, at least for samples $> 100 \text{ \AA}$ in thickness. One would expect that if the profile has distinct regions that are due to separate surface and volume populations, the relative size of the volume contribution would increase as the sample thickness increased. The fact that it does not suggest that the distribution of sites is in fact a characteristic of the entire ice sample. This is potentially consistent with an ice that is highly microporous, like the structure of a sponge, so that the "surface" does in fact dominate the population for all our experimental thicknesses. If amorphous water ice has such an open structure, adsorbed molecules in the volume of the ice would be in equilibrium with those in

the gas phase. As such, H_2 molecules would freely migrate between the gas phase and the porous ice volume until finding a vacant binding site. We tried to test this experimentally, with a sequenced deposition of H_2O and H_2 . The deposited H_2O was allowed to sit for several hours so that the cryopumping of H_2O had effectively stopped. The H_2 was then deposited on this water substrate. Our results suggest that to within a factor of two, this gives the same $112/1120$ ratio as our codepositional experiments. However, the results of this sequence experiment were not as clear or reproducible as our other experiments. We hope to repeat this set of experiments in the near future, to properly assess the nature of the amorphous ice surface.

A previous explanation for the temperature-dependent release of H_2 from a water ice matrix has been put forward by Laufer et al. (1987). They concluded that the 112 is physically trapped in the water ice during codeposition. As the water ice matrix is heated, this opens the ice structure in a steady and repeatable way, which controls the release of trapped $1-12$. This would imply that the population of trapped H_2 is dictated by conformational changes in the water only. Large trapped abundances are then probably an artifact of the fast laboratory deposition rates. This would suggest that accretional trapping is a minor effect under interstellar conditions. *Our intent is to offer the alternative explanation that the population of H_2 in the ice samples may be an equilibrium situation, controlled primarily by the thermodynamic behavior of a simple distribution of binding site energies.*

5. THE H_2 ABUNDANCE IN INTERSTELLAR, ALI GRAIN MANTLES

The amount of H_2 incorporated in interstellar grain mantles dominated by water ice can be derived from this physical model of an equilibrium between gas phase H_2 and the grain binding site energy distribution. Utilizing the concept of a

critical binding energy, the respective gas-grain collision frequencies under laboratory and interstellar conditions allow a direct comparison of the population of adsorbed H_2 in these two environments. Following the procedure outlined above to determine the critical binding energy of an ice surface at a given temperature and under a given number density of H_2 , we can estimate this value for various interstellar conditions, where molecular hydrogen also dominates the available gas phase speciation, typically by several orders of magnitude. $E_b(\text{crit})$ then fully determines the equilibrium fractional abundance of bound H_2 for the grain mantle. For example, at reasonable molecular cloud values of $T = 10 \text{ K}$ and $n(\text{H}_2) = 10^4 \text{ cm}^{-3}$, $E_b(\text{crit}) \sim 450 \text{ K}$. For this value, the equilibrium population of H_2 will fill over 90% of the available surface sites in the theoretical surface distribution. As we postulate that $\sim 80\%$ of the desorbed H_2 in our experiments is due to a similar equilibrium population, and that the total $\text{H}_2/\text{H}_2\text{O}$ ratio in our samples is 0.53, we estimate that interstellar grains have an $\text{H}_2/\text{H}_2\text{O}$ ratio as high as $-(0.9)(0.8)(0.53) \sim 0.4$. The equilibrium fractional abundance of H_2 in a grain mantle dominated by H_2 and H_2O would then be ~ 0.3 . Adding any deeply buried, non-equilibrium H_2 will only raise this abundance, Figure 5 summarizes calculated values of $E_b(\text{crit})$ and the corresponding predicted fractional abundance of H_2 in grain mantles for different values of interstellar gas-grain temperature and gas phase H_2 number density. For comparison with the interstellar results, the derived values of $E_b(\text{crit})$ and fractional H_2 abundances from our codeposition experiments with different substrate temperatures are also shown in Fig. 5. Note that at low temperatures, in particular, the higher gas phase densities in the laboratory relative to typical interstellar conditions do not lead to significant differences in the equilibrium fractional H_2 abundances, as $E_b(\text{crit})$ is not a sensitive function of gas phase number density. Thus in the context of the equilibrium model, our laboratory provides a reasonable simulation of the interstellar environment.

This equilibrium model may adequately describe the observed interstellar frozen H_2 abundance along the line of sight of WL5 in the p Oph molecular cloud (Sandford et al. 1993). WL5 is a deeply embedded infrared source ($A_v \geq 50$), with local number densities thought to be in the range of 10^4 - 10^6 cm^{-3} (Wilking and Iada, 1983). The detection of pure CO ice along this line of sight (Kerr, Adamson, & Whittet 1991) indicates that temperatures must be below 25 K, probably in the range of 10-25 K. Plotting this range of conditions in Fig. 5, we predict that grain mantles along this line of sight would have H_2 fractional abundances from 0.05 to 0.30. Unfortunately, an observational determination of the ratio of H_2 to total ice molecules toward WL5 has not been made. The column abundance of water ice along this line of sight is uncertain, as the observed water ice feature at 3.1 μm is saturated (Tanaka et al. 1990). However, the ice phase $\text{H}_2/\text{CH}_3\text{OH}$ ratio has been determined to be ≤ 0.08 (Sandford et al. 1993). Given that the 1120/3130 μm ratio is ~ 2 - 3 as it is for ices in other similar interstellar environments, and that these two species likely dominate the composition of most grain mantles (Allamandola, Sandford, & Tielens 1992), this would put the fractional abundance of H_2 along this line of sight at the few percent level, consistent with the lower end of our predicted range.

If this equilibrium model is correct, molecular hydrogen in interstellar grains would be a widespread phenomenon. Ultraviolet photoprocessing would not be a requirement to explain the presence of frozen H_2 in interstellar ices. We suggest, then, that interstellar grains may have a significant fractional abundance of 1-12% ($\sim 30\%$ of the total number density) at 10 K temperatures even in unilluminated regions of molecular clouds. The presence of H_2 as a product of photolysis in the ice would be a special case limited only to regions with a significant UV flux. More observations of the frozen H_2 feature along other lines of sight with widely varying UV radiation

budgets are needed to adequately test the relative importance of UV photoprocessing versus gas phase accretion.

Significant quantities of molecular hydrogen incorporated in the icy mantles of interstellar grains will clearly affect grain chemistry and physics. Molecular hydrogen would fill the most energetic sites on the grain surface, leaving only weak sites for the physisorption of other molecules. Heavy chemical species will be bound less strongly to, and desorb more easily from, an H₂ rich ice (Allen & Robinson 1977) predicting less depletion of heavy species onto grains. Atomic and molecular mobility over the surface of amorphous ice mantles will be very different if the ice surface is saturated with H₂ (Smoluchowski 1983). One would intuitively expect that the surface mobility of other species would increase, as only the least energetic sites would be available. This could possibly enhance chemical reaction rates on grain surfaces, although surface abundances and the residence time scales for species heavier than H₂ would be lowered.

If the volume of icy grain mantles are also rich in H₂, this should provide a more reducing environment for energetic reactions in the mantle, such as those occurring in ice irradiation experimental simulations (see, for example, Greenberg et al. 1993; Pirronello 1993; and references therein). This is interesting in light of the reported production of H₂ in ultraviolet photolysis experiments on icy interstellar mixtures (Sandford & Allamandola 1993). The presence of large amounts of H₂ in such an ice from adsorption may suppress such reactions, as the addition of product molecules would shift the chemical equilibrium to favor larger abundances of the reactant species. In addition, the overall increase in the ice mantle number density due to the bound H₂ should result in a higher heat capacity of the grain mantle than in previous estimates, thereby changing our understanding of mantle heating processes.

As comets are thought to be largely aggregates of interstellar icy grains, a truly primitive, unprocessed comet should reflect the composition of its interstellar origin. A primitive comet composed of ices that had never experienced temperatures above 20 K might then have a large amount of hydrogen incorporated in its bulk. Comets composed of icy material that had experienced higher temperatures would show a diminished amount of hydrogen in accordance with the amounts shown in Figure 5. The total amount of molecular hydrogen incorporated in a comet might then provide a sensitive test of the degree of thermal processing that a comet, or the much smaller grains that accumulate to form comets, had experienced since the ice had originally condensed.

6. CONCLUSIONS

Our experimental results show that codeposition of H_2 with H_2O at 12 K can incorporate a large fraction of hydrogen in the water matrix, up to a molar $\text{H}_2/\text{H}_2\text{O}$ ratio of 0.53. Nearly 80% of this population of H_2 sublimates at temperatures below 30 K, while the remainder appears stable well above 40 K. The more volatile component is consistent with an equilibrium distribution of surface binding site energies, described theoretically by Hixson et al. (1992). Such an explanation would predict molar abundances of H_2 in interstellar grain mantles of nearly 0.3 due only to the accretion of gas phase molecular hydrogen. For the probable conditions of W15 in the ρ Ophiuchi cloud, fractional H_2 abundances of between 0.05 and 0.3 are calculated from the equilibrium model, in possible agreement with the observed abundance (Sandford et al. 1993).

To adequately test if this process can explain the recent detection of frozen H_2 in interstellar ices, more work is needed on laboratory, theoretical, and observational

fronts. Laboratory work is required to definitively establish whether our results are either due to an equilibrium bound population of H_2 , or mechanical matrix trapping of H_2 by the water deposition. Such work needs to be understood in detail if the results are to be extrapolated to interstellar conditions. Experimental work is also needed to determine if other common interstellar ices, such as CO or CH_3OH , have the same ability to adsorb a large fraction of H_2 as water ice. The modeling must also substantially improve, to determine how the potential energy surface of a simulated amorphous water cluster changes as more molecular hydrogen is added. Additional work also is needed to predict the likelihood and relative energies of sites deep within an ice volume. Finally, the observational detection of solid phase H_2 in interstellar space demands more such work along many different lines of sight. The generality of this feature is key to our understanding of the processes which may yield H_2 in interstellar grain mantles.

ACKNOWLEDGEMENTS

This work represents research carried out at the Jet Propulsion Laboratory, California Institute of Technology, under contract to the National Aeronautics and Space Administration. One of us (RWD) would like to thank the NASA Graduate Student Researchers Program for their support. The comments of G. Blake, W. Langer, and M. Werner are appreciated,

REFERENCES

- Allamandola, L. J., Sandford, S. A., & Tielens, A. G. G. M. 1992, *Ap. J.*, 399, 134.
- Allamandola, L. J., Sandford, S. A., & Valero, G. J. 1988, *Icarus*, 76, 225.
- Allen, M., & Robinson, G. W. 1976, *Ap. J.*, 207, 745.
- Allen, M., & Robinson, G. W. 1977, *Ap. J.*, 212, 396.
- Dissly, R. W., Allen, M., & Anicich, V. G. 1992, *BAAS*, 24, 1120.
- Govers, T. R., Mattera, L., & Stoles, G. 1980, *Chem. Phys.*, 72, 5446.
- Greenberg, J. M., Mendoza-Gomez, C. X., de Groot, M. S., & Breukers, R. 1993, in *Dust and Chemistry in Astronomy*, ed. T. J. Millar & D. A. Williams (Philadelphia: Bristol), 271.
- Hixson, H. G., Wojcik, M. J., Devlin, M. S., Devlin, J. P., & Buch V. 1992, *J. Chem. Phys.*, 97, 753.
- Hollenbach, D., & Salpeter, E. E. 1970, *Chem. Phys.*, 53, 79.
- Kerr, T. H., Adamson, A. J., & Whittet, D. C. B. 1991, *MNRAS*, 251, 60p.
- Laufer, D., Kochavi, E., & Bar-Nun, A. 1987, *Phys. Rev. B*, 36, 9219.
- Lee, T. J. 1972, *Nature*, 237, 99.
- Lee, T. J., Gowland, I., & Reddish, V. C. 1971, *Nature*, 231, 193.
- Mayer, E., & Pletzer, R. 1986, *Nature*, 319, 298.
- Pirronello, V. 1993, in *Dust and Chemistry in Astronomy*, ed. T. J. Millar & D. A. Williams (Philadelphia: Bristol), 297.
- Sandford, S. A., & Allamandola, L. J. 1993, *Ap. J. (Letters)*, 409, 65.
- Sandford, S. A., Allamandola, L. J., & Geballe, T. R. 1993, *Science*, 262, 400.
- Smoluchowski, R. J. 1983, *J. Chem. Phys.*, 87, 4229.

- Solomon, P. M., & Wickramasinghe, N. C. 1969, *Ap. J.*, 158,449.
- Tanaka, M., Sata, S., Nagata, T., & Yamamoto, "I". 1990, *Ap. J.*, 352,724.
- Tielens, A. G. G. M., & Allamandola, L. J. 1987, in *Interstellar Processes*, ed. D. J. Hollenbach & H. A. Tronson, Jr. (Dordrecht:Reidel), 397.
- Tielens, A. G. G. M., & Hagen, W. 1982, *A&A*, 114,245.
- Wickramasinghe, N. C., & Reddish, V. C. 1968, *Nature*, 218, 661.
- Wilking, B. A., & Iada, J. 1983, *Ap. J.*, 274,698.

Figure Captions

Figure 1- The total abundances of H_2 and H_2O in ice samples deposited on a sapphire substrate cooled to 12 K. The filled squares represent codepositions of H_2 and H_2O , prepared with $\text{H}_2:\text{H}_2\text{O}$ gaseous inlet pressures between 4:1 and 36:1, with deposition times between 20 minutes and 2.5 hours. Deposition of pure H_2O is indicated by the open circle, and deposition of pure H_2 is represented by the open diamond. The open triangle represents an ice sample allowed to sit in the chamber for several hours after deposition while H_2O cryopumped from other parts of the vacuum chamber onto the sample, and the open square represents an identically deposited sample allowed to sit several hours, but now under an atmosphere of 10^{-5} torr of H_2 maintained in the chamber. The dashed line shows the best fit for the ratio $\text{H}_2/\text{H}_2\text{O}$ of 0.53.

Figure 2- Resorption profiles for H_2 and H_2O during heating of ice samples at a steady rate of 2 K/min. Ice samples were prepared under identical conditions, but at different window substrate temperatures. H_2 resorption profiles for window temperatures of 12 K, 20 K, and 30 K are indicated by open squares, diamonds, and triangles, respectively. The desorption profile of H_2O from the 12 K deposition is indicated by filled circles. Lines between markers serve only to aid visualization, and do not represent actual data. The H_2 resorption profiles for the 20 K and 30 K depositions were normalized by setting the H_2O abundance from these samples equal to that of the water abundance in the 12 K deposition.

Figure 3-1-12 resorption profile (open circles) for a temperature programmed resorption experiment. The heating profile is indicated by the dashed line. The $\text{H}_2/\text{H}_2\text{O}$ ice mixture was prepared under the same conditions as the experiments

shown in Figure 2, with a window temperature of 12 K. Again, the line between markers serves only as a visualization aid.

Fig. 4- Comparison of our experimental results with a theoretical distribution of surface binding site energies, given by Hixson et al. (1992). Values are presented as $f(E_b)$, the fraction of sites with E_b greater than a given value. The filled squares represent the theoretical distribution. The open squares represent the distribution of H_2 binding site energies derived from the TPD experiment (Fig. 3). The open circles represent a similar distribution inferred from the results for depositions at 12, 20, and 30 K (Fig. 2). Errors were determined relative to the normalized abundances at 380 K, the minimum value of binding energy for H_2 that we could feasibly detect (see text). Again, lines between markers serves only as a visualization aid.

Figure 5- Critical binding energies and equilibrium fractional H_2 abundances in interstellar grain mantles for different H_2 gas phase number densities and gas-grain temperatures. The solid lines show calculated $E_b(\text{crit})$ values at 10, 20, 30, and 40 K. The H_2 fractional abundances of 0.01, 0.1, 0.2, and 0.3 are indicated (dashed lines) for the appropriate values of $E_b(\text{crit})$. The open circle represents the value of $E_b(\text{crit})$ computed for the conditions in the cloud containing W15, as described in the text. The filled circles show $E_b(\text{crit})$ for laboratory conditions at a background pressure of $\sim 3 \times 10^{-8}$ torr and ice temperatures of 12, 20, 30, and 40 K. Their slight offset from the isothermal lines is due to $E_b(\text{crit})$ being determined for a 300 K gas phase temperature.

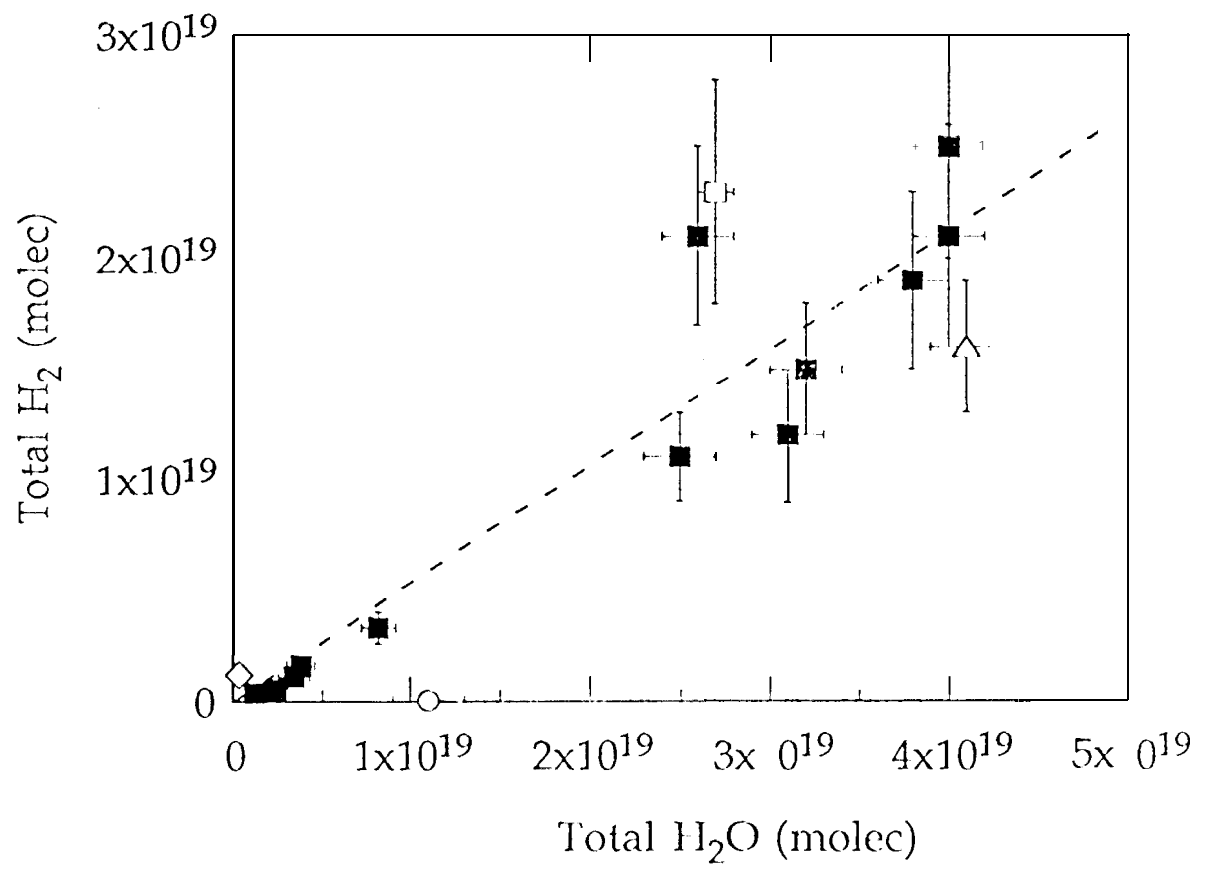


Figure 1

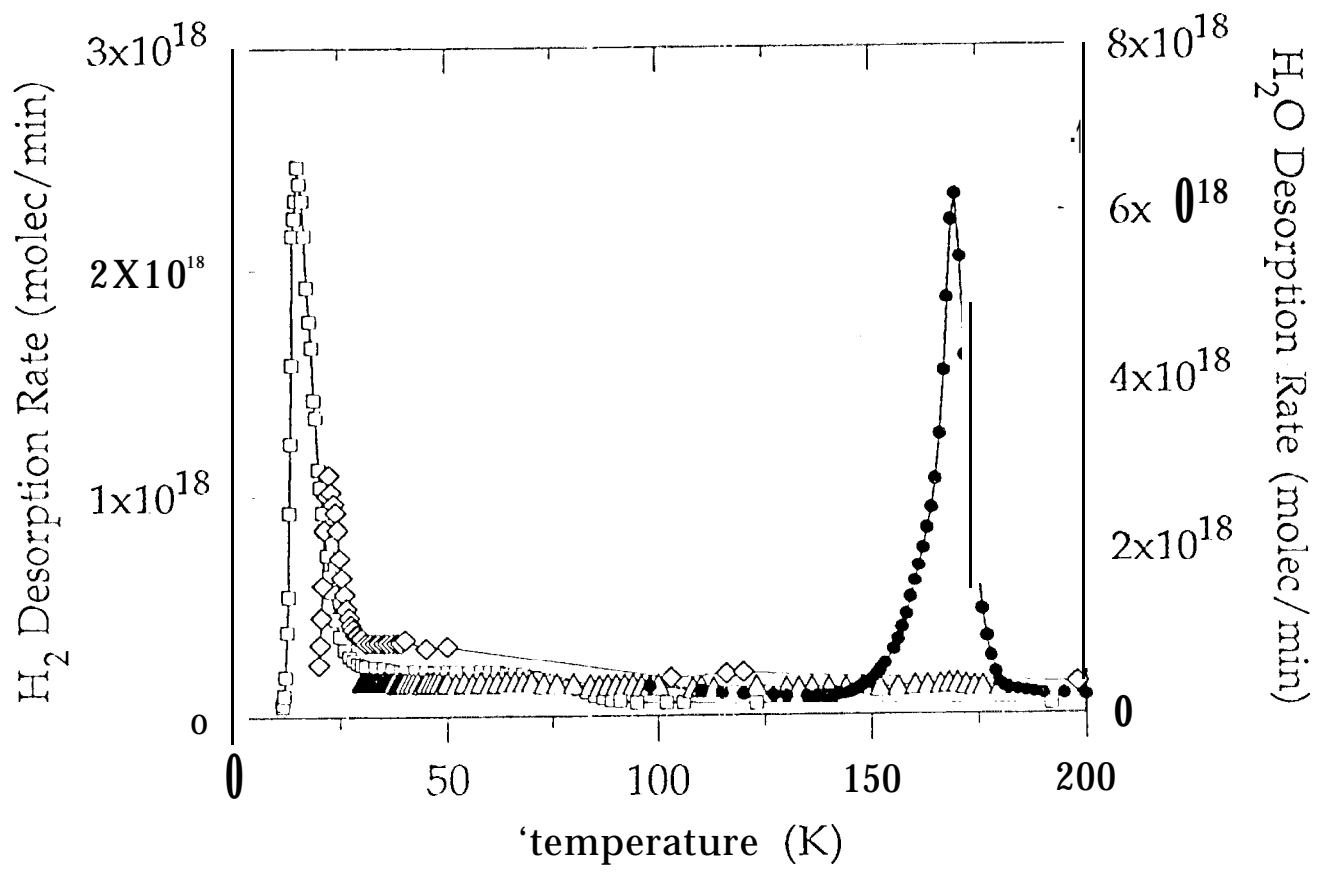


Figure 2

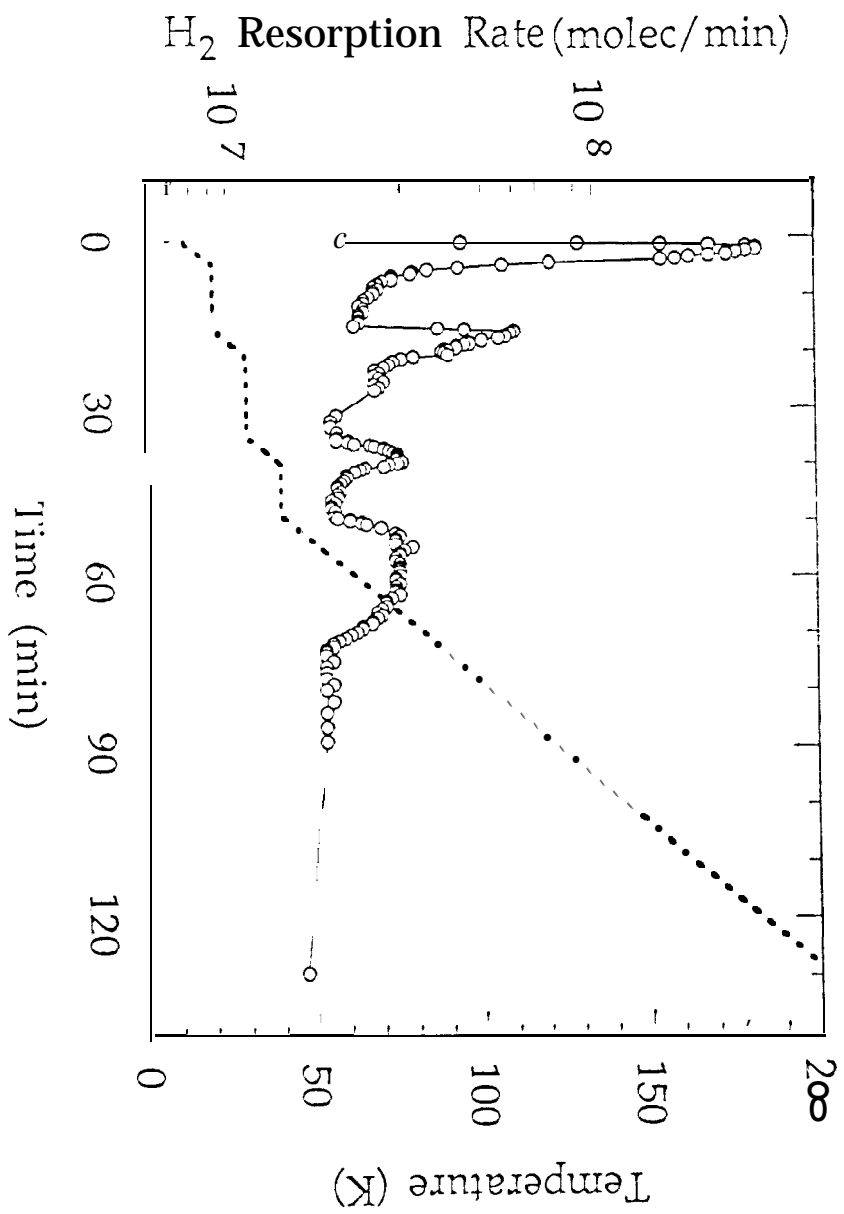


Figure 3

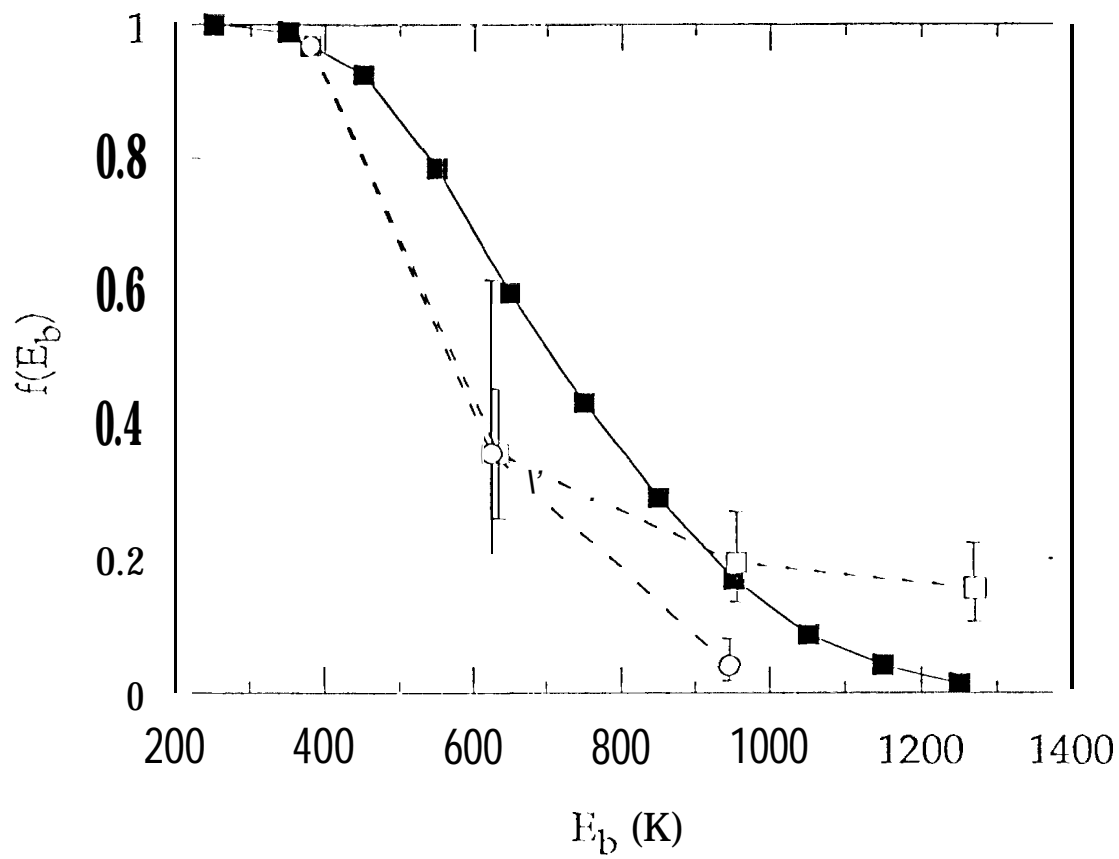


Figure 4

